

CuO-TiO₂ as a visible light responsive photocatalyst for the photoelectroreduction of CO₂ to methanol

Kaykobad Md. Rezaul Karim¹, Mariotte Anak Patrick Jebi¹, Huei Ruey Ong², Hamidah Abdullah¹, Mostafa Tarek¹, Chin Kui Cheng¹, Md. Maksudur Rahman Khan^{1,3*}

¹Faculty of Chemical and Natural Resources Engineering, Universiti Malaysia Pahang, Lebuhraya Tun Razak, 26300 Kuantan, Pahang, Malaysia.

²Faculty of Engineering and Technology, DRB-HICOM University of Automotive Malaysia, 26607 Pekan, Pahang, Malaysia.

³Centre of Excellence for Advanced Research in Fluid Flow (CARIFF), University Malaysia Pahang, 26300 Kuantan, Pahang, Malaysia.

*E-mail: mrkhancep@yahoo.com, Tel. +6095492872, fax: +6095492889

Abstract - As rising atmospheric CO₂ levels change Earth's climate change, CO₂ reduction has become an increasingly active area in energy research over the past several years. The present work is developing artificial photosynthesis technologies that use visible light to convert CO₂ and water into methanol. In this study, TiO₂ loaded copper oxide (CuO-TiO₂) was synthesized, characterized and studied for photoelectrochemical (PEC) reduction of CO₂ into methanol under visible light ($\lambda > 470$ nm) irradiation. In this perspective, the catalyst was synthesized via Sol-gel method. Catalyst characterization was done by X-ray diffraction (XRD), X-ray photoelectron spectroscopy (XPS), UV-vis absorption spectra, and Mott-Schottky (MS). Linear sweep voltammetry (LSV) was employed to evaluate the photocatalytic activity of the prepared photocatalyst under visible light ($\lambda > 420$ nm) irradiation for CO₂ reduction reactions. XRD results indicated that the particle size of the as-prepared photocatalyst was 65 nm. The oxidation state of Cu²⁺ and Ti⁴⁺ were confirmed by XPS results. The band gap of CuO-TiO₂ composite characterization results indicated that the band gap energy of the CuO-TiO₂ catalyst was 1.68 eV. The flat band potential was calculated from the MS data and was found at 0.83 V vs NHE. During LSV, the onset potential was shifted positively (~100 mV) under the light on condition than the dark condition in CO₂ saturated solution suggests an increase in photocurrent and occurrence CO₂ photoreduction reaction. The PEC performance of CuO-TiO₂ photocatalyst showed an increased methanol formation and found the optimum yield of 20.1 $\mu\text{mol.L}^{-1}\text{cm}^{-2}$ under visible light irradiation.

Keywords: CO₂ reduction; Photoelectrochemical; visible light; CuO-TiO₂ photocathode; methanol

1. INTRODUCTION

The rapid emissions of CO₂ in atmospheric posed one of the most crucial issues with regard to the greenhouse effect. This issue has raised multiple concerns to find different CO₂ mitigation technologies and strategies into a clean energy fuel. The mimic photosynthesis process has sparked a new sustainable development way in recent years in order to solve major issues nowadays: climate change and energy shortage, which can be implemented using water (H₂O) as both proton and electron supply photoreduction of H₂O and CO₂ into hydrocarbons fuels [1] The idea of converting CO₂ to hydrocarbons is originates from natural photosynthesis process which produce carbohydrate and oxygen from H₂O and CO₂, via the harvest and exploitation of solar energy. However, since CO₂ is chemically stable, the conversion of CO₂ is quite difficult without the assistance of any catalyst and requires large energy input [2]. In this research area, solar photocatalytic reduction of CO₂ has been extensively investigated. Generally, photocatalysis (PC) requires photoresponsive materials capable of harvesting solar light to produce photogenerated electrons and enable to transfer multiple electrons for the formation of different products. Although photocatalysis is the most promising solutions but typically suffers from mechanistic complexity, poor product selectivity and slow kinetics[3]. The one electron reduction of CO₂ to generate CO₂⁻ is not easily possible because in the reduction of CO₂ the first electron transfer to generate CO₂⁻ requires nearly -1.90 V vs NHE and it is an uphill process with great over potential. Thus, a novel light-driven and electrically biased PEC cell as the combination of electrocatalysis and photocatalysis is one of the key improvement to overcome the low product selectivity and reduce energy input over photocatalyst (Li, et al., 2015).

Toward this artificial photosynthesis, the photocatalyst is typically a hybrid material capable of produce photogenerated electrons by absorbs visible light. The photogenerated electrons are separated and reached in the catalyst surface and offer active sites for further catalytic reaction. [4]. TiO_2 is one of the optimistic photocatalysts due to its excellent properties, such as high stability, non-toxicity and low cost and [5]. However, it was known that TiO_2 (band gap 3.2 eV) is a UV light-driven photocatalyst limited to a high e^-/h^+ recombination rate [6]. On the other hand, semiconductors suffer from low quantum efficiencies and selectivity due to the formation of H_2 in an aqueous solution simultaneously during CO_2 reduction. H_2 formation reaction is the main competitive reaction which should be suppressed to produce a selective product during the CO_2 reaction. Artificial photosynthesis could be achieved by using an appropriate photocathode for CO_2 reduction. In order to solve low quantum yield and selectivity problems, multiple attempts on band gap tuning to make TiO_2 active for visible light photocatalyst by introducing defects with transition metals. In CO_2 reduction, the addition of TiO_2 cocatalysts has been investigated including RGO- Cu_2O [7], N_2 doped TiO_2 [8] and $\text{Cu}_x\text{O-TiO}_2$ [9]. Thus, helped to improve electron-hole separation and act as sink onto photocatalyst surface and to improve the photocatalytic efficiency. At hybrid $\text{Cu}_x\text{O-TiO}_2$ heterostructured composite a remarkable methane formation was observed during CO_2 reduction and found as 221.63 ppm $\text{g}^{-1}\text{h}^{-1}$. The photocatalytic CO_2 reduction efficiency of Cu_2O can be improved by coupling Cu_2O with TiO_2 , acting as a charge transfer enhancing layer [9].

To the best of our understanding, so far there was no information in the literature on CuO-TiO_2 catalyst for photoelectroreduction of CO_2 to liquid products under visible light irradiation. Another approach is to couple TiO_2 to CuO , a p-type semiconductor can exist in different stoichiometry and phases such as Cu_2O and CuO with narrow band gap energy from 1.2 to 2 e.V. The band gap energy ($E_g = 1.35\text{--}1.7$ eV) of CuO lies near the CO_2/O_2 potential and are used as a visible light active photocatalyst [10]. Thus, CuO-TiO_2 represent one of the most appealing systems and is expected to produce an enhanced charge carrier lifetime, with beneficial impact both on catalytic performance [11]. Therefore, this study is to synthesise and characterizes CuO-TiO_2 as a visible light responsive photocatalyst that used in CO_2 photoelectrochemical reduction into methanol under solar light irradiation. The catalyst was characterized by using UV-Vis, XRD and XPS. The photoelectrochemical behaviour of the catalyst for CO_2 reduction was evaluated by LSV and MS analysis.

2. EXPERIMENTAL

A. Materials and Methods

Copper (II) nitrate trihydrate, $\text{Cu}(\text{NO}_3)_2 \cdot 3\text{H}_2\text{O}$ (99%) (2.3 g), titanium (IV) dioxide, TiO_2 (99%) (2.53 g), hydrazine monohydrate, $\text{N}_2\text{H}_4 \cdot \text{H}_2\text{O}$ (0.347 M), ascorbic acid and NaHCO_3 are of the analytical condition and used without extra purification.

B. Preparation of CuO-TiO_2

The CuO-TiO_2 was prepared by Sol-gel method. A required amount of $\text{Cu}(\text{NO}_3)_2 \cdot 3\text{H}_2\text{O}$ and TiO_2 Degussa-P25 powder, and ascorbic acid (0.02M) were dispersed into the solution of 50 ml distilled water. After that, 11 mL of $\text{N}_2\text{H}_4 \cdot \text{H}_2\text{O}$ (0.347 M) act as reducing agent was added into the reaction mixture with continuous stirring at room temperature for ~ 4 h until colour changes from blue to red precipitate (Ramli, et al., 2014). The paste sample was then dried at 70°C , 0.5 MPa in a vacuum oven for overnight. Finally, the sample was grinded into a fine powder using marble mortar.

The electrodes were prepared with the method described by Woon et al., Ong et al. [12], [13]. Briefly, the catalyst ink was prepared by mixing 22 mg of CuO-TiO_2 with 140 μL of 5 wt% Nafion and 280 μL isopropanol ($\text{C}_3\text{H}_8\text{O}$) followed by ultrasonication for 30 min. Thereafter, the ink was evenly brushed with an area of 1 cm^2 of graphite paper. The electrode was dried in vacuum oven at 90°C for 6 h.

C. Catalyst characterization

X-ray diffraction (XRD) was performed by Rigaku Mini Flex II (30 kV and 15 mA), Japan to determine the broadening of the diffraction peak of the prepared catalysts. The specimens will be step-wise scanned over the operational range of scattering angle (2θ) between 10° to 80° , with a scan step of $0.02^\circ/\text{min}$. The data were recorded in terms of the diffracted X-ray intensity (I) versus 2θ . Ultraviolet-visible (UV-NIR) absorption spectroscopy was conducted by Shimadzu UV-2600. XPS study was performed using a VG Microtech MT500 with an Mg-K α X-ray source. MS experiment was done at 2000 Hz frequencies by using an electrochemical analyser (Autolab Compact PGSTAT 204, Netherland) with an Ag/AgCl electrode, CuO-TiO_2

electrode and platinum foil used as a reference electrode, working electrode and counter electrode respectively in 0.1 M NaHCO_3 aqueous solution (pH 6.8)

D. Photoelectrochemical measurement

All PEC reduction of the CO_2 study were performed in a single chamber PEC cell equipped with a quartz window reactor as illustrated in Figure 1. All the PEC measurement were completed by using a potentiostat (Autolab Compact PGSTAT 204, Netherland) using a typical three electrode-system consists of Ag/AgCl electrode, CuO-TiO₂ electrode and platinum foil used as a reference electrode, working electrode and counter electrode respectively in 0.1 M NaHCO_3 aqueous solution (pH 6.8). Prior to start the reaction, high purity CO_2 (99.99%) gas was purged in to the 0.1M NaHCO_3 aqueous solution for 30 min at a fixed flow rate so that the concentration of CO_2 into the solution reached saturation. LSV was carried out from the potential range of -0.2 to -0.8 V vs NHE with 10 mV/s scan rate. Light irradiation (Light source: XD-300 High Brightness Cold Light Source, Beijing Perfect light Co., Ltd., China,) was kept constant during LSV scanning light on the condition. For product analysis, 5 mL of aqueous reaction sample was withdrawn at a different time interval and was quantified by DB-WAX 123-7033 column (30 m x 0.32 mm x 0.5 μm) in GC-FID equipped with 7694 E headspace autosampler injection for methanol (CH_3OH) analysis.

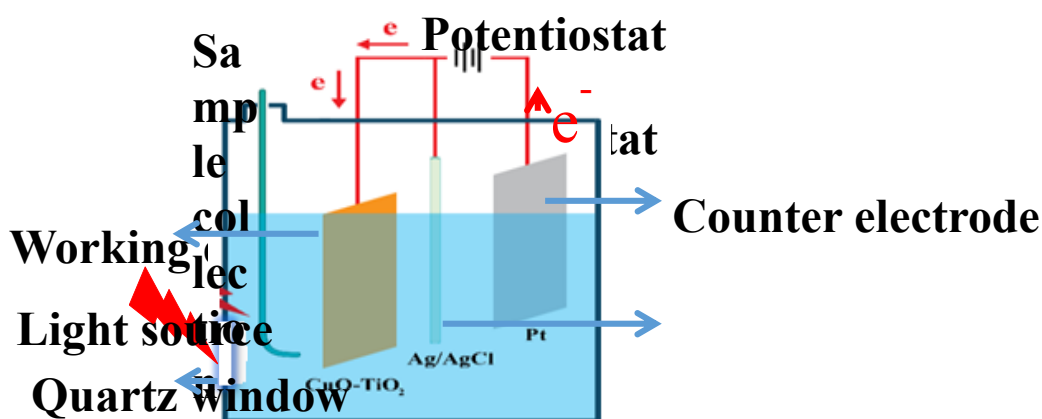


Figure1: Schematic diagram of PEC reduction of CO_2 on CuO-TiO₂

3. RESULTS AND DISCUSSION

A. Characterization of CuO-TiO₂

Figure 2(a) depicted the absorbance chart for wavelength 200 to 900 nm which shows the visible light response capacity of the prepared photocatalysts. The band gap of the as-prepared catalysts was determined by using the $\alpha\nu$ plot as shown in Figure 2 (b) which represents the indirect transition of band gap energy values by plotting $(\alpha\nu)^{1/2}$ versus $h\nu$. The band gap of the commercial TiO_2 was found 3.3 eV which correspond to wavelength absorption of 397 nm and the CuO-TiO₂ with a higher intensity of absorption displayed lower optical band gap energy of 1.68 eV as expected for CuO according to literature reports [14]. When a metal or compound is loaded to the other catalyst, the previous band gap may be shifted to a new band gap. Commercial TiO_2 can be used as an effective bandgap modifier to absorb the light ranging under the visible light region [9]. Therefore, the as-prepared CuO-TiO₂ composite catalysts with low band gap can be able to enhance the photoabsorption capacity towards the visible light region.

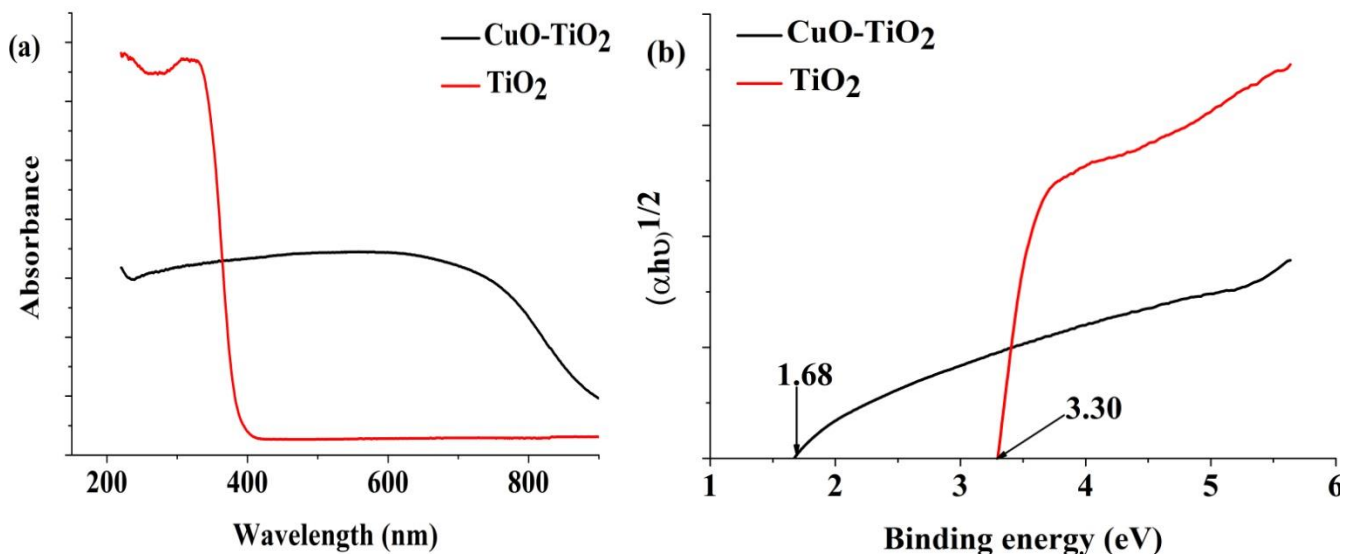


Figure 2: (a) UV-Vis spectrum of CuO-TiO₂ (b) Tauc plot for band gap energy calculation of as-prepared photocatalysts.

Figure 3 shows the XRD pattern of the as-prepared CuO-TiO₂. From the JCPDS Card No. 45-937 database, all the diffraction peak position of can be indexed as monoclinic CuO phase (Barreca, et al., 2011). In particular, the patterns showed the reflections peaks on $2\theta = 32.44^\circ, 38.72^\circ, 48.7^\circ, 53.40^\circ, 58.25^\circ, 66.20^\circ, 72.4^\circ,$ and 75.2 can be easily indexed to (110), (111), (202), (320), (321), (410), (511) and (622) crystal planes, respectively (JCPDS Card No. 45-937) with lattice parameters $a_0 = 4.684, b_0 = 3.425$ and $c_0 = 5.129 \text{ \AA}$. The peaks matching well with the anatase TiO₂, the relative peak around at $35.09^\circ, 61.61^\circ,$ and 67.48° are indexed to the diffraction of the (311), (422) and (611) plane of the TiO₂ indicating that TiO₂ and CuO coexist in the CuO-TiO₂ heterojunction. This is understandable because the lattice constants of anatase TiO₂ are similar to those of CuO [15] Therefore, from diffraction pattern it can be concluded that crystalline CuO on TiO₂ has been formed.

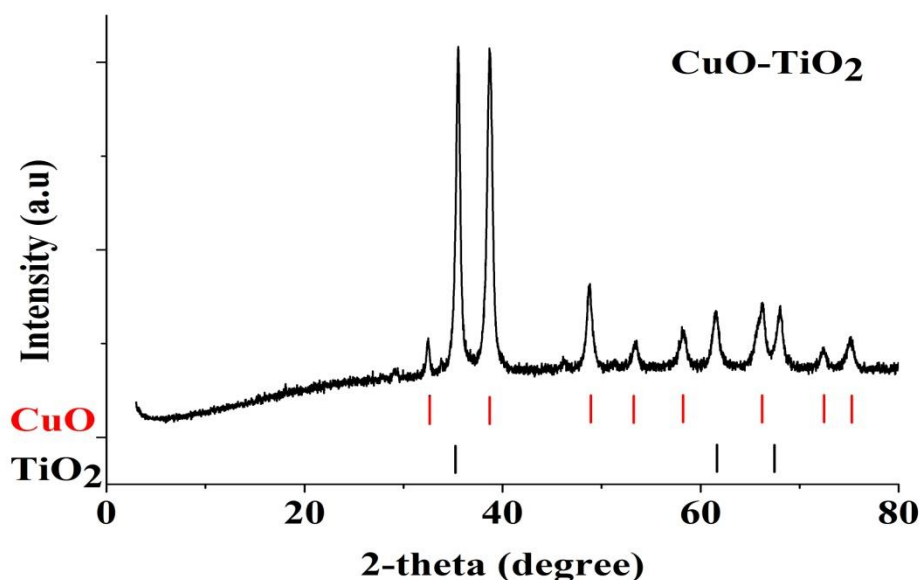


Figure 3: XRD patterns on the as-prepared CuO-TiO₂

XPS was done to identify the oxidation state of Cu and Ti on CuO-TiO₂ composite catalyst. The XPS spectra of Cu2p Figure 4(a) demonstrate the existence of Cu2p_{1/2} (binding energy at 951.9 eV) and Cu2p_{3/2} (binding energy at 932.2 eV). Furthermore, shake-up peak at 942.8 eV and 940.6 eV are indicative of the presence of Cu²⁺ in the composite catalyst. The XPS spectra of Ti in Figure 4 (b) shows three peaks at 461.5 eV, 456.09 eV and 452.2 eV. The first peak is assigned for Ti2p_{1/2} whereas the other two peaks are assigned for for Ti2p_{3/2} (Park, et al., 2016). The o 1s spectrum shown in figure 4(c) shows a major peak at 530.0 eV matches to O²⁻ in CuO and TiO₂ and a secondary peak at 531.0 eV is assigned to the oxygen species adsorbed on the surface [16].

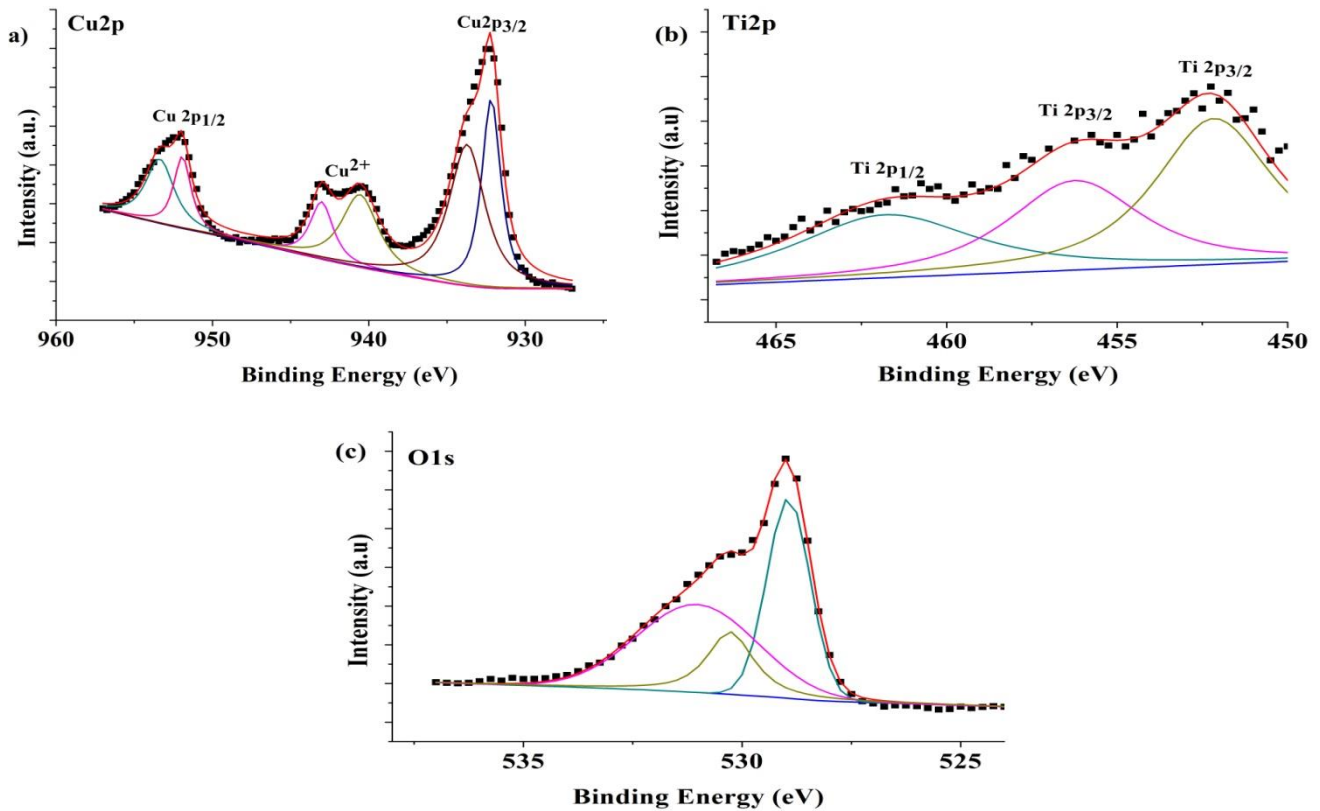


Figure 4: XPS spectra for (a) Cu2p and (b) Ti2p and (c) O 1s in CuO-TiO₂

To find out the valence band position of the prepared catalyst, the Mott-Schottky analysis was carried out in 0.1 M NaHCO₃ solutions (pH 6.8) shown in Figure 5 (a). Flat band potential (E_{fb}) is normally situated close to the VB, and it can be calculated from the intersection of a plot of $1/C^2$ against E by the following equation 1 [17]:

$$\frac{1}{C^2} = \frac{2}{e \epsilon \epsilon_0 N} \left(E - E_{fb} - \frac{kT}{e} \right) \dots \dots \dots (1)$$

where C , e , ϵ , ϵ_0 are the capacitance, electron charge, dielectric constant and permittivity of vacuum respectively, whereas the N , E , E_{fb} , k and T are the acceptor density, electrode potential, flat band potential, Boltzmann constant, and temperature respectively. Figure 5a shows that the x-axis intercept was 0.80 V vs NHE. The flat band potential was calculated using the equation (1) and found 0.83 V vs NHE. Figure 5b displays the band diagram for CuO-TiO₂ and the thermodynamic redox potential of CO₂ reduction (V vs NHE). The calculated VB and CB potential of CuO-TiO₂ were approximately -0.83 and -0.85 V versus an NHE, respectively. Due to a higher CB of CuO-TiO₂ than that of the redox potential of CO₂, the excited electrons in the CB can be easily used by the CO₂ molecules and converted to its reduced products. Moreover, with the assistance of an external bias potential electron-hole recombination rate will be low leading to the efficient photoelectrochemical reduction of CO₂ [18].

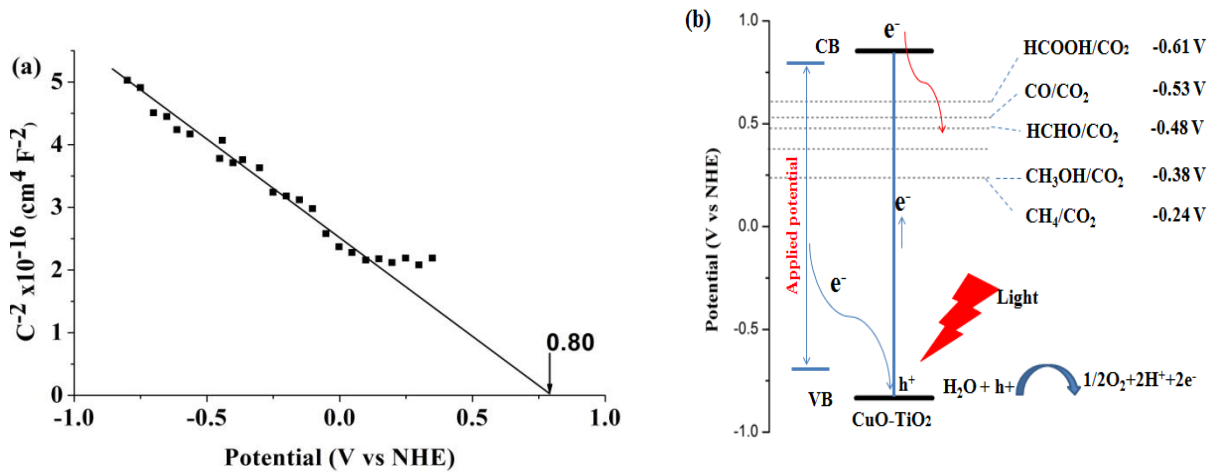


Figure 5: (a) Mott-Schottky plot of CuO-TiO₂ at 2000 Hz (b) Position of the conduction band and valence band of CuO-TiO₂ photocathode together with the redox potential of various reduction products at pH 6.8.

B. Photoelectrochemical performance

Figure 6 depicted the LSV for CuO-TiO₂ in 0.1M NaHCO₃ solution with the N₂-saturated and CO₂-saturated solution under dark and visible light illumination at scan rate 10 mV/s. Higher reduction photocurrent under CO₂-saturated than under a N₂-saturated environment was observed, indicating the CO₂ reducibility of CuO-TiO₂ under the light on condition.. The cathodic current was increased as the applied potential increased for light on compared to light off condition. This phenomenon might be due to water/proton reduction [19]. In contrast, it was observed that with light irradiation, the cathodic current profile for CuO-TiO₂ was improved with the copper loading with onset potential value from -0.2V with maximum current at -0.8V versus NHE. A remarkable shift of onset potential to the positive region, indicating the reaction could occur with less applied potential in presence of light.

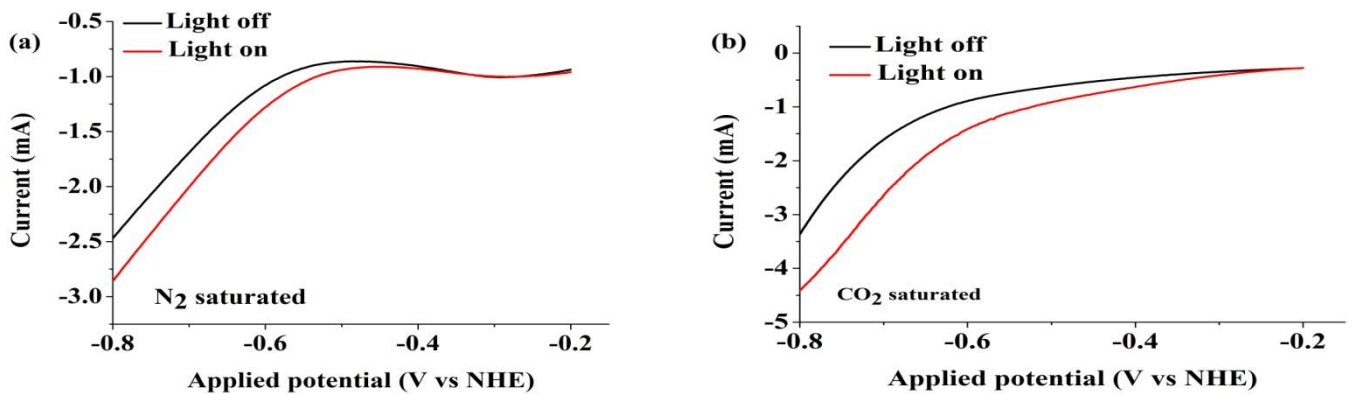
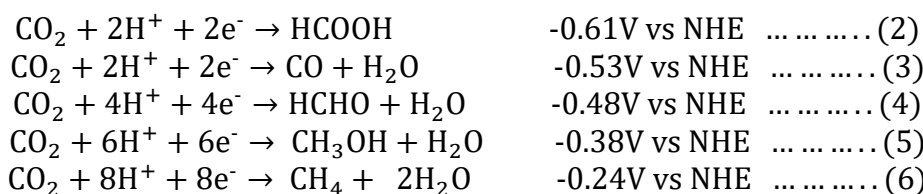


Figure 6: LSV of CuO-TiO₂ electrode N₂-saturated and CO₂-saturated 0.1 M NaHCO₃ solution under light on/off (scan rate 10 mV/s; light wavelength = 470 nm)

Proton-coupled multiple electron reduction reactions may occur over CuO-TiO₂ during CO₂ followed 2e⁻, 4e⁻, 6e⁻ and 8e⁻ pathway [20] can be described in Eqs. (2-6):



The PEC, EC and PC reduction of CO₂ were conducted in 250 ml of CO₂-saturated 0.1 M NaHCO₃ solution at -0.36 V vs NHE under 470 nm wavelength irradiation for 4 hr (Figure7). In this work, methanol was found as the main product in the liquid phase as analysed in GC-FID. It was found out that during the blank experiment (only 0.1M NaHCO₃ solution without CO₂ purging), no other C1 products obtained, proving that carbon in CH₃OH originated from the purged CO₂. With CuO-TiO₂ electrode, the methanol yield increased as irradiation time progressed. At 4 h reaction time, amount of methanol yield for PC, EC and PEC was monitored to be 2.35, 15.40 and 20.1 μmol.L⁻¹.cm⁻² respectively. Moreover, the resulting methanol yield in PEC system was better compared to the summation of EC and PC (17.75 μmol.L⁻¹.cm⁻²) processes on CuO-TiO₂ confirming the synergistic effect in term of product yield.

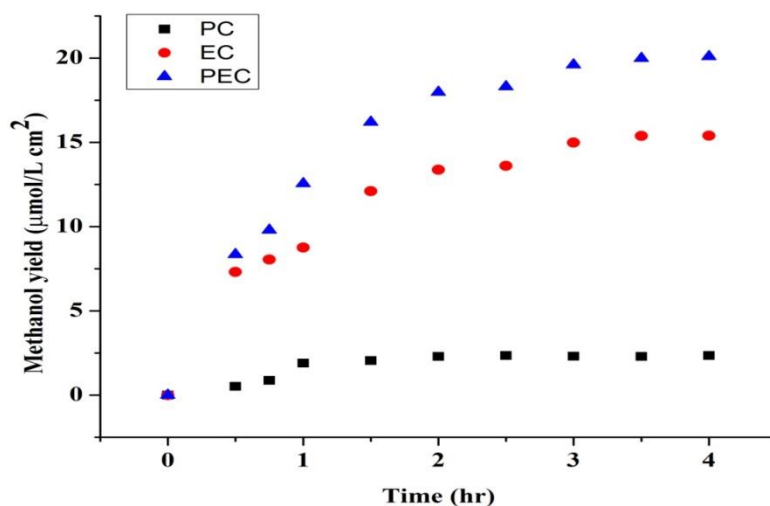


Figure7: Methanol yields under photoelectrocatalytic (PEC), electrocatalytic (EC) and photocatalytic (PC) conditions with reaction time over CuO-TiO₂ electrode.

Based on the above results, a possible mechanism was proposed for the PEC reduction of CO₂ to methanol in figure 8. Within the CuO-TiO₂ photocatalyst, the electrons (e⁻) and holes (h⁺) recombination process were inhibited by applying external bias potential. Upon light driven, photoelectrons generated from CuO-TiO₂ at VB jumps to CB, and promote the flows to CO₂ due to the band bending between the interface of the photocatalyst. To activate the inert CO₂ molecule for reduction, the best way is to absorb it on the surface of CuO-TiO₂ catalyst electrode. If a high-dielectric-constant solvent is used such as water, the CO₂⁻ anion radicals can be greatly stabilized by the solvent, resulting in weak interactions with the photocatalyst surface. After the adsorption, upon visible light irradiation, electrons and holes are produced and reaction initiates. Electron reached to the adsorbed CO₂ and reduced it to an anion radical ⁻CO₂ whereas, H₂O oxidation proceeds through the holes, which make H⁺, O₂ and excited electrons, which is being participated in the reaction. The H⁺ further takes electrons and form [•]H, which reacts with the ⁻CO₂ to make CO and OH⁻.

The CB of CuO-TiO₂ was -0.77 V vs NHE which was more negative than the reduction potential of CO₂/CH₃OH (-0.38 V vs. NHE), indicating that the prepared catalyst has enough PC to reduce CO₂ to CH₃OH. Besides this, the externally applied bias potential could not only improve the parting of electrons and holes to improve the CO₂ reduction capacity but also supplied additional electrons to keep up the EC reduction of CO₂. However, the efficiency of the reaction could be low, due to the electron-hole (e⁻/h⁺) recombination process. Therefore, at minimum potentials of -0.36 V vs NHE, can assist CO₂ reduction and is important for selective product production. The PEC result was compared with EC and PC system possesses two advantages: (i) the applied bias potential not only assists selective reaction but also enhances the partition of photoinduced charge carriers, enhancing PEC process; (ii) Visible light irradiation lowers the required potential for CO₂ reduction and promotes the electrode kinetics for a selective product, favouring the EC process thus capable to reduce CO₂ to CH₃OH [21].

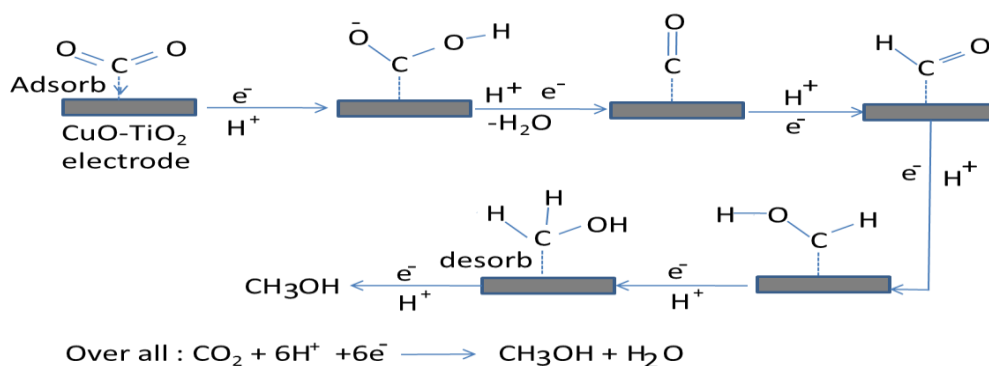


Figure 8: Scheme of CO₂ photoreduction mechanism on CuO-TiO₂ catalyst

4. CONCLUSION

The photoelectrocatalytic reduction of CO₂ in an aqueous solution under visible light irradiation was carried out successfully in the as-prepared CuO-TiO₂ composite catalyst prepared by Sol-gel method. The characterization results showed that the loading of CuO on TiO₂ reduced the band gap thus increased visible light absorption by shifting the band-gap of commercial TiO₂ (3.3 eV) into a new band gap of CuO-TiO₂ (1.68 eV). The VB and CB position of CuO-TiO₂ was -0.83 V and -0.85 V versus a NHE, respectively that calculated from UV-Vis and Mott-Schottky result. Methanol yield in PEC system was found higher (20.1 μmol.L⁻¹.cm²) than PC and EC reaction system over CuO-TiO₂. The higher yield of methanol in PEC may be occurred due to the synergistic effect. An electron flow scheme was proposed to demonstrate the possible CO₂ reduction reaction. The separation of photo-induced carrier and hole was more effective under applied bias potential, and it enabled more photoelectrons availability at the surface CO₂ reduction active sites. Thus, further research is required to explore the effect of CuO loading on TiO₂ and mechanism phenomena for CO₂ reduction by PEC and understand the CO₂ reduction mechanism in depth.

ACKNOWLEDGMENT

The authors would like to thank Universiti Malaysia Pahang (www.ump.edu.my) for research grants (RDU172202 and PGRS170353) and the Malaysian Ministry of Higher Education for Fundamental Research Grant Scheme (RDU 150118).

REFERENCES

- [1] T. Arai, et al., "Selective CO₂ conversion to formate in water using a CZTS photocathode modified with a ruthenium complex polymer," *Chemical Communications*. 2011. **47**(47): p. 12664-12666.
- [2] A. Sarkar, et al., "Photocatalytic reduction of CO₂ with H₂O over modified TiO₂ nanofibers: Understanding the reduction pathway," *Nano Research*. 2016. **9**(7): p. 1956-1968.
- [3] W. Tu, Y. Zhou, Z. Zou, "Photocatalytic Conversion of CO₂ into Renewable Hydrocarbon Fuels: State-of-the-Art Accomplishment, Challenges, and Prospects," *Advanced Materials*. 2014. **26**(27): p. 4607-4626.
- [4] J. Jiao, et al., "Photocatalysts of 3D Ordered Macroporous TiO₂-Supported CeO₂ Nanolayers: Design, Preparation, and Their Catalytic Performances for the Reduction of CO₂ with H₂O under Simulated Solar Irradiation," *Industrial & Engineering Chemistry Research*. 2014. **53**(44): p. 17345-17354.
- [5] S. A. Ansari, et al., "Gold nanoparticles-sensitized wide and narrow band gap TiO₂ for visible light applications: a comparative study," *New Journal of Chemistry*. 2015. **39**(6): p. 4708-4715.
- [6] B. Fang, et al., "Hierarchical CuO-TiO₂ Hollow Microspheres for Highly Efficient Photodriven Reduction of CO₂ to CH₄," *ACS Sustainable Chemistry & Engineering*. 2015. **3**(10): p. 2381-2388.
- [7] X. An, K. Li, J. Tang, "Cu₂O/Reduced Graphene Oxide Composites for the Photocatalytic Conversion of CO₂," *ChemSusChem*. 2014. **7**(4): p. 1086-1093.
- [8] M. S. Akple, et al., "Nitrogen-doped TiO₂ microspheres with enhanced visible light photocatalytic activity for CO₂ reduction," *Chinese Journal of Catalysis*. 2015. **36**(12): p. 2127-2134.
- [9] S. M. Park, et al., "Hybrid Cu_xO-TiO₂ Heterostructured Composites for Photocatalytic CO₂ Reduction into Methane Using Solar Irradiation: Sunlight into Fuel," *ACS Omega*. 2016. **1**(5): p. 868-875.
- [10] S. I. In, D. D. Vaughn, R. E. Schaak, "Hybrid CuO-TiO₂-xNx Hollow Nanocubes for Photocatalytic Conversion of CO₂ into Methane under Solar Irradiation," *Angewandte Chemie International Edition*. 2012. **51**(16): p. 3915-3918.

- [11] D. Barreca, et al., "Novel Synthesis and Gas Sensing Performances of CuO–TiO₂ Nanocomposites Functionalized with Au Nanoparticles," *The Journal of Physical Chemistry C*. 2011. **115**(21): p. 10510-10517.
- [12] C. W. Woon, et al., "MnO₂/CNT as ORR Electrocatalyst in Air-Cathode Microbial Fuel Cells," *Procedia Chemistry*. 2015. **16**: p. 640-647.
- [13] M. R. Khan, et al., "Nanostructured Pt/MnO₂ Catalysts and Their Performance for Oxygen Reduction Reaction in Air Cathode Microbial Fuel Cell," *International Journal of Electrical, Computer, Electronics and Communication Engineering*. 2015. **9**(3): p. 247–253.
- [14] S. J. A. Moniz, J. Tang, "Charge Transfer and Photocatalytic Activity in CuO/TiO₂ Nanoparticle Heterojunctions Synthesised through a Rapid, One-Pot, Microwave Solvothermal Route," *ChemCatChem*. 2015. **7**(11): p. 1659-1667.
- [15] N. Thi Hiep, et al., "Synthesis and characterization of nano-CuO and CuO/TiO₂ photocatalysts. *Advances in Natural Sciences*," *Nanoscience and Nanotechnology*. 2013. **4**(2): p. 025002.
- [16] Z. Jin, et al., "Photo-reduced Cu/CuO nanoclusters on TiO₂ nanotube arrays as highly efficient and reusable catalyst," 2017. **7**: p. 39695.
- [17] S. Kamimura, et al., "Fabrication and characterization of a p-type Cu₃Nb₂O₈ photocathode toward photoelectrochemical reduction of carbon dioxide," *Applied Catalysis B: Environmental*. 2015. **174**: p. 471-476.
- [18] J. Gu, et al., "Mg-Doped CuFeO₂ photocathodes for photoelectrochemical reduction of carbon dioxide," *The Journal of Physical Chemistry C*. 2013. **117**(24): p. 12415-12422.
- [19] Q. Shen, et al., "High-yield and selective photoelectrocatalytic reduction of CO₂ to formate by metallic copper decorated Co₃O₄ nanotube arrays," *Environmental science & technology*. 2015. **49**(9): p. 5828-5835.
- [20] E. E. Benson, et al., "Electrocatalytic and homogeneous approaches to conversion of CO₂ to liquid fuels," *Chemical Society Reviews*. 2009. **38**(1): p. 89-99.
- [21] X. Huang, et al., "Synergistic Photoelectrochemical Synthesis of Formate from CO₂ on {12 $\bar{1}$ } Hierarchical Co₃O₄," *The Journal of Physical Chemistry C*. 2013. **117**(50): p. 26432-26440.